Trichroic Infrared Studies of Oriented Nylon 11

Hsin Her Yu and Leslie J. Fina*

Department of Mechanics and Materials Science, College of Engineering, Rutgers—The State University, P.O. Box 909, Piscataway, New Jersey 08855-0909

Received February 4, 1994; Revised Manuscript Received June 23, 1994®

ABSTRACT: An investigation of the orientation of the amide groups and the methylene spacers in oriented Nylon 11 films has been undertaken using trichroic Fourier transform infrared spectroscopy. Phenomena that are investigated include sample drawing, electric field application, and annealing. The results show that the overall sample symmetry is greater than uniaxial for all samples studied. In the drawn film the hydrogen-bonded sheets show a tendency to locate in the plane of the film, while the orientation of the hydrocarbon segments is random around the chain axis. The methylene segments are found to be randomly oriented about their chain axes as a result of drawing and poling treatments and become slightly ordered with annealing. Least-squares Gaussian curve-fitting is used to separate the amide I region into four peaks, allowing for the orientation of ordered and disordered amide groups to be followed. Whereas the disordered amide groups show little or no preferred orientation about the chain axis independent of sample treatment, the ordered amide groups show substantial orientation for all sample treatments. The ordered amide planes tend to align in the plane of the film with one-way drawing. After annealing of drawn films, the width of the orientation distribution of ordered amide planes narrows but keeps the plane of the film as the distribution center. As a result of the poling of drawn films, ordered amide domains switch toward the field direction. Dipole polarization mechanisms of 60° and 90° are considered to account for the effect of the electric field. In samples which were drawn, poled, and then annealed, the ordered part of the amide groups does not move toward the thickness direction, but rotates back to the plane of the film.

Introduction

Nylon 11 can exist in at least five crystal forms.[1-5] Of these, two are triclinic (α and α') and three are pseudohexagonal (γ, δ, and δ'). Melt-quenching and subsequent cold-drawing of Nylon 11 results in a pseudohexagonal form which displays piezoelectric properties.[6,7] Wide-angle X-ray diffraction conducted in the reflection mode shows that the crystallinity increases and the *d* spacing between the hydrogen-bonded sheets reduces with annealing treatments for drawn films.[7] A preferred alignment of the hydrogen-bonded sheets was found in melt-quenched, drawn, and then annealed samples.[8] In addition, after comparison of the X-ray diffraction patterns of drawn plus annealed films with drawn, poled, and then annealed films, a 90° field-induced dipole reorientation mechanism was inferred.[9] It would be a benefit to examine diffraction patterns before annealing treatments in order to determine polarization switching and annealing mechanisms directly. Differences in the X-ray diffraction patterns occur between drawn and drawn plus poled films in the absence of annealing treatments. However, unannealed films possess diffuse X-ray patterns which are difficult to analyze. Infrared spectroscopy is used in this study to examine the orientational response of disordered and ordered fractions of Nylon 11 both before and after annealing treatments.

Infrared spectroscopy used in the transmission mode provides information about the components of transition dipole moments which occur in the plane perpendicular to the direction of light propagation. When the sample symmetry is higher than uniaxial, an alternate means must be used to obtain absorption information in three dimensions. Two methods that have been extensively used are trichroic infrared and attenuated total reflection spectroscopy. The former method is based on sample tilting with respect to the incident light direction,[10-13] and the latter, on the fact that electric field components exist in all three directions of space for parallel and perpendicularly polarized light.[14] Trichroic infrared analysis has been used in the past to study the orientation in three dimensions of drawn and annealed poly(vinylidene fluoride) (PVF_2).[13] In this work it was found that in drawn PVF_2 films, the CF_2 dipoles preferentially orient around the chain axes of *all-trans* conformational sequences. The preferred orientation remained in tact with annealing treatments close to the melt, suggesting a crystalline origin. A similar phenomenon was found at the surface of drawn Nylon 11 films using ATR spectroscopy.[14] In that work, the amide planes were found to be well-oriented and primarily reside in the plane of the film as a result of simple one-way drawing of unoriented melt-quenched samples. Room temperature poling treatments showed minor effects in the amide plane orientation due to the surface specificity of ATR. The purpose of the present work is a more thorough trichroic infrared investigation of the orientation of the amide planes and the methylene spacers in one-way drawn films of Nylon 11. The trichroic infrared intensities are used to follow the preferential orientation of groups around the chain axis in response to drawing, annealing, and poling treatments.

Experimental Section

Sample Preparation. The Nylon 11 powder used in this study was provided by the Rilsan Corp. (Glen Rock, NJ). Films are prepared by melting the powder between aluminum foil sheets in a hot press at 210 °C, followed by quenching into an ice water bath. After removing the aluminum foil sheets by physical separation, all films are uniaxially stretched to a draw ratio of 3:1 at room temperature. The final thickness of the oriented films is in the range 4.5–5.9 μm. For poling treatments gold is evaporated on both sides of the films to a thickness of approximately 200 Å. The area of the electrodes is 80 mm^2. Films are poled by a triangular electric pulse with a period of 640 s and a maximum amplitude of 150 MV/m under "degassed" conditions; i.e., the sample was poled inside a desiccant container filled with silicon oil which had been purged with dry air. Each sample was cycled six times from +150 to −150 MV/m, producing a constant remanent polarization. Two sets of films are annealed under vacuum for 2 h at 180 °C at constant strain: drawn films and drawn plus poled films. The infrared spectra of all drawn films

* To whom correspondence should be addressed.
® Abstract published in *Advance ACS Abstracts*, August 15, 1994.

0024-9297/94/2227-6192$04.50/0

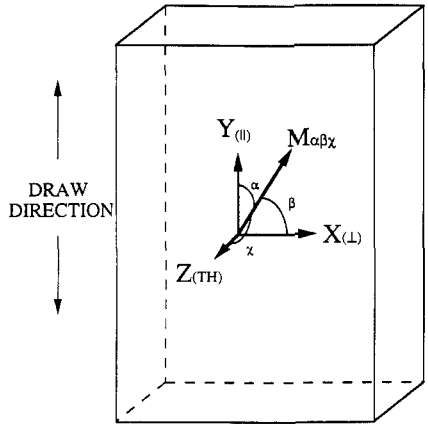

Figure 1. Location of the film in a Cartesian coordinate system with a representative transition dipole moment (M) at angles α, β, and χ from the axis system.

are collected before postdrawing treatments so that spectral changes as a result of the treatments can be directly interpreted, i.e., independent of initial thickness variations.

Infrared Spectroscopy. Infrared spectra are collected with either a Digilab Model FTS-60A or a Perkin-Elmer 1750 Fourier transform infrared spectrometer equipped with a TGS detector at a resolution of 2 cm^{-1}. Three-dimensional absorption data are generated by sample tilting. The sample is mounted on a movable stage, which could be rotated around the horizontal or vertical axis. A Perkin-Elmer wire grid polarizer is placed after the sample to collect polarized spectra. The sample and background are scanned 200 times. A Balston dry air purge is employed to remove atmospheric moisture. All spectra are stored and processed on a VAX Cluster.

Results

The spectra in the parallel (draw direction) and perpendicular (in the plane of the film) can be measured directly by using polarized light alternately positioned at 0 and 90° to the draw direction. In order to obtain the thickness direction spectrum, a polarized normal incidence and a tilted-film spectrum must be combined with the refractive index of the film.[10,11] The refractive index and the thickness of the isotropic unoriented Nylon 11 films in the infrared frequency range are estimated to be 1.515 and 4.45 μm, respectively, using a nonlinear least-squares fitting procedure of the interference fringe pattern in the regions of nonabsorption for a film cast from trifluoroacetic acid. Using a birefringence of 0.04,[15] the refractive index in the parallel and perpendicular directions of the stretched film is found to be 1.545 and 1.505, respectively.

The thickness direction spectrum (A_z) is calculated using[11]

$$A_z = \frac{A_{\alpha,\beta,\chi}\left(1 - \frac{\sin^2\alpha}{n^2}\right)^{1/2} - A_y}{\left(\frac{\sin\alpha}{n}\right)^2} + A_y \qquad (1)$$

where $A_{\alpha,\beta,\chi}$ is the polarized tilted absorption spectrum, α is the tilt angle, n is the refractive index, and A_y is the untilted polarized absorption spectrum. Equation 1 can be used to calculate A_z by rotation of the film around either the X- or Y-axis, as shown in Figure 1. In practice, the Y-axis is coincident with the drawn direction and the A_z spectrum is found by tilting around the X-axis. This treatment leads to a considerably better signal-to-noise ratio in the A_z spectrum as compared to tilting around the Y-axis.

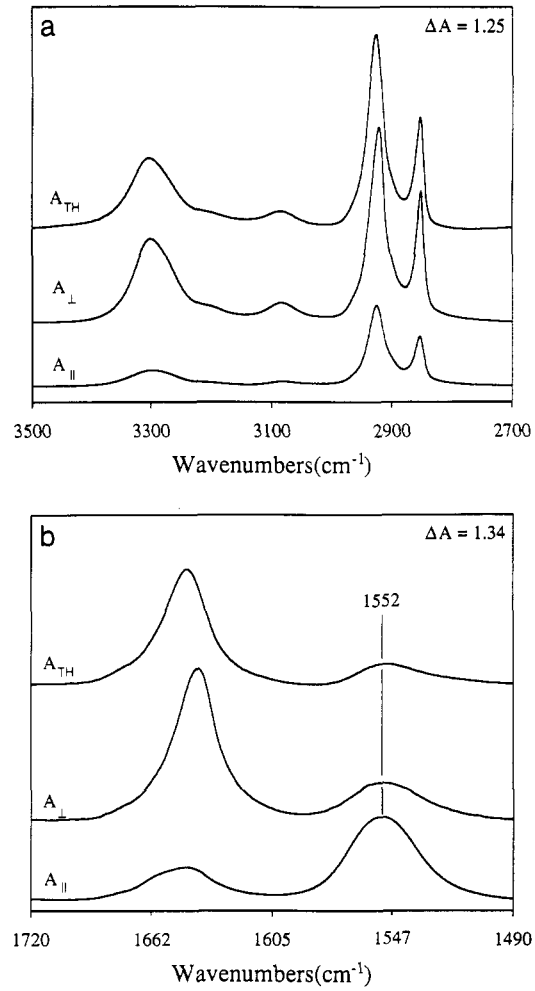

Figure 2. (a) Parallel, perpendicular, and calculated thickness direction infrared absorption spectra for a one-way drawn Nylon 11 film in the region 3500–2700 cm^{-1}. (b) Same as Figure 2a in the region 1720–1490 cm^{-1}.

Infrared spectra of the three orthogonal directions: parallel, perpendicular, and thickness for a drawn Nylon 11 film are shown in Figure 2 in the methylene/N—H stretching (Figure 2a) and amide I/II (Figure 2b) regions. The band at ca. 3300 cm^{-1} (amide A peak) is assigned to hydrogen-bonded N—H stretching modes. Two strong bands at ca. 2920 and 2850 cm^{-1} are assigned to the antisymmetric and symmetric CH_2 stretching modes of the methylene groups, respectively. The amide I mode is composed primarily of a carbonyl stretching motion (77–80%) with smaller contributions from the C—N stretching and the N—H in-plane bending and is associated with the 1645 cm^{-1} band.[16,17] The amide II mode is composed of the N—H in-plane bending (43–60%) and the C—N stretching (26–40%) with smaller possible contributions from C$^{\alpha}$—C and N—C$^{\alpha}$ stretching and is located at ca. 1550 cm^{-1}.[16,17] In Figure 2 the intensity differences between the parallel and the other two directions is a result of chain alignment in the draw direction. The peak positions of the amide A and amide I modes for drawn Nylon 11 are shown in Table 1 and indicate that the hydrogen bond strength is anisotropic in three directions. On the basis of the frequency and intensity data, it can be established that the amide groups in one-way drawn films with transition dipole moment components in the plane transverse to the draw direction are more highly ordered in the perpendicular (X) direction.

A comparison of the spectra of drawn plus annealed films, Figure 3, with that of drawn films, Figure 2, shows

Table 1. Observed Frequencies of Nylon 11

vibrational mode		∥	⊥	TH
N—H(ν)[a]	drawn	3295.8 ± 0.9[b]	3297.8 ± 1.2	3301.6 ± 1.2
(amide A)	poled	3296.8 ± 0.6	3300.4 ± 0.3	3303.6 ± 0.7
	pol + ann	3305.3 ± 0.8	3304.1 ± 0.4	3308.0 ± 0.1
	annealed	3303.9 ± 0.5	3304.4 ± 0.2	3306.4 ± 0.4
$CH_2(\nu_a)$	drawn	2923.8 ± 0.1	2921.4 ± 0.2	2925.0 ± 0.2
	poled	2924.0 ± 0.1	2921.1 ± 0.3	2924.0 ± 0.1
	pol + ann	2924.1 ± 0.1	2919.9 ± 0.3	2922.8 ± 0.1
	annealed	2924.1 ± 0.1	2920.0 ± 0.1	2923.0 ± 0.3
$CH_2(\nu_s)$	drawn	2852.1 ± 0.1	2850.7 ± 0.1	2852.2 ± 0.1
	poled	2852.2 ± 0.1	2850.8 ± 0.1	2851.7 ± 0.1
	pol + ann	2852.2 ± 0.1	2850.6 ± 0.1	2851.4 ± 0.1
	annealed	2852.2 ± 0.1	2850.2 ± 0.1	2851.6 ± 0.1
amide I	drawn	1644.8 ± 0.4	1640.4 ± 0.3	1645.4 ± 0.3
	poled	1645.3 ± 0.1	1640.3 ± 0.1	1644.8 ± 0.1
	pol + ann	1645.7 ± 0.4	1637.1 ± 0.2	1643.4 ± 0.1
	annealed	1646.0 ± 0.3	1636.7 ± 0.4	1642.4 ± 0.1
amide II	drawn	1552.3 ± 0.5	1551.0 ± 0.1	1552.8 ± 0.8
	poled	1551.9 ± 0.3	1551.8 ± 0.1	1550.7 ± 0.7
	pol + ann	1544.3 ± 0.2	1549.7 ± 0.3	1546.3 ± 2.8
	annealed	1544.6 ± 0.1	1548.2 ± 0.1	1549.4 ± 0.3

[a] N—H(ν) = N—H stretch; $CH_2(\nu_a)$ = antisymmetric methylene stretch; $CH_2(\nu_s)$ = symmetric methylene stretch. [b] Errors are the standard deviation of several experimental runs.

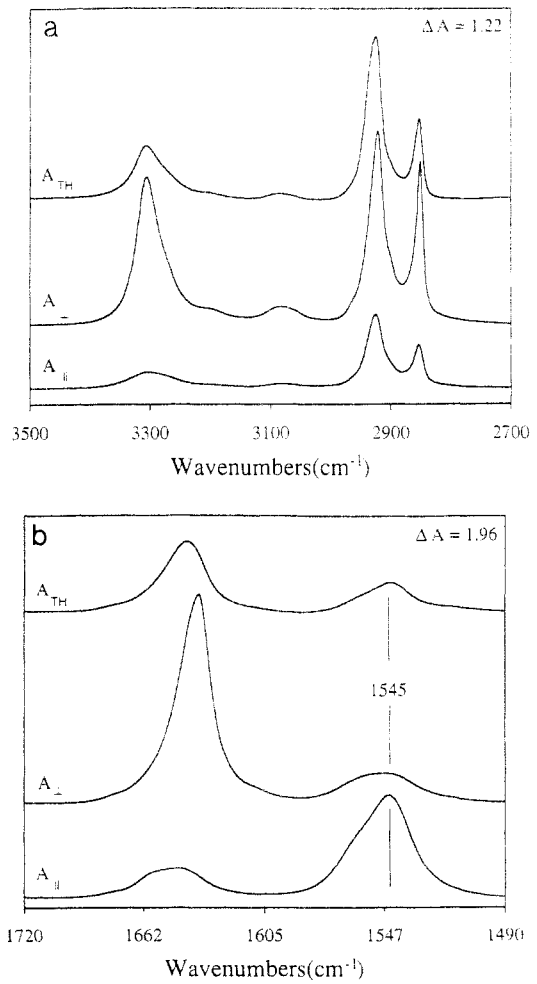

Figure 3. (a) Three-dimensional infrared spectra of a drawn plus annealed Nylon 11 film in the region 3500–2700 cm^{-1}. (b) Same as Figure 3a in the region 1720–1490 cm^{-1}.

that annealing causes the amide A and amide I peak half-widths to decrease. Additionally, the intensity of the perpendicular direction peaks becomes much larger than the thickness. When the direction of the transition moment of these modes with respect to the amide plane is considered, i.e., approximately parallel to it, these changes establish that the average amide plane moves toward the plane of the film with annealing treatments. An examination of the influence of annealing on the amide A peak in Table 1 reveals that the frequency *increases* in all directions as compared to the drawn film's frequencies. This behavior establishes that the average strength of the hydrogen bonds after annealing of drawn films is weaker than in drawn films and therefore that the average N—H to C=O distance is greater. This unexpected observation will be discussed later. We also note in Figure 3a that the amide A peak has a noticeable low-frequency asymmetry, particularly in the parallel direction, but also present in the perpendicular and thickness directions. In the past this shoulder has been assigned to the amide I overtone in Fermi resonance with the amide A mode.[18] The spectra of annealed films will be further considered in the Discussion.

The change of the amide I frequencies due to annealing in Table 1 shows that the parallel direction increases in frequency by 1.1 cm^{-1}, the perpendicular direction decreases by 3.7 cm^{-1}, and the thickness direction decreases by 3.0 cm^{-1}. Since the peak frequency of the amide I mode is a function of the relative amount of ordered, disordered, and free carbonyl groups,[19] annealing greatly improves the hydrogen bond ordering in the plane transverse to the draw direction. The dipoles that have non-zero projections on the parallel direction after annealing are more disordered. Two driving forces are active during the annealing process, the maximization of hydrogen bond strength and the tendency to establish crystal-like ordering. The increase in the amide A frquencies coupled with a decrease in the amide I frequencies suggests that the tendency to form crystal ordering is the stronger of the two.

The amide II peak (ca. 1550 cm^{-1}) increases slightly in intensity in the parallel direction relative to the other two directions as a result of annealing and shows a large peak frequency decrease. The frequency change is related to a crystal phase change which occurs with annealing; i.e., pseudohexagonal δ-structures transform to α-structures.[20,21] On the other hand, the intensity increase in the parallel direction with annealing is indicative of either the preferential formation of α-structures with their amide II transition moments aligned in the parallel direction or a tilting of amide planes toward the draw direction with annealing.

Polarization measurements in Nylon 11 exhibit electric displacement (D) versus electric field (E) hysteresis loops, as typically found in ferroelectric materials. Figure 4 shows an example of the D–E curve for the sixth and last ac cycle with the currently used poling procedure. The remanent polarization (P_r) and the coercive field (E_c) were determined from the figure by the intercept of the loop with the D- and E-axes, respectively, as P_r = 53.2 mC/m^2 and E_c = 55.5 MV/m.

The three-dimensional spectra for a drawn plus poled film are shown in Figure 5. The bands at ca. 3300 and 1650 cm^{-1} show direct evidence for the poling process when compared with Figure 2. Both peaks show a decrease in intensity in the perpendicular direction and an increase in the thickness direction. Inspection of the frequency of the amide II mode in Figures 2b and 5b and in Table 1 shows that a crystal phase transformation does not occur as a result of electric field treatments. A significant point concerning the methylene groups is that the orientation around their chain axes is not affected by the poling process, indicated by the lack of change in the methylene stretching mode intensities between Figures 2a and 5a.

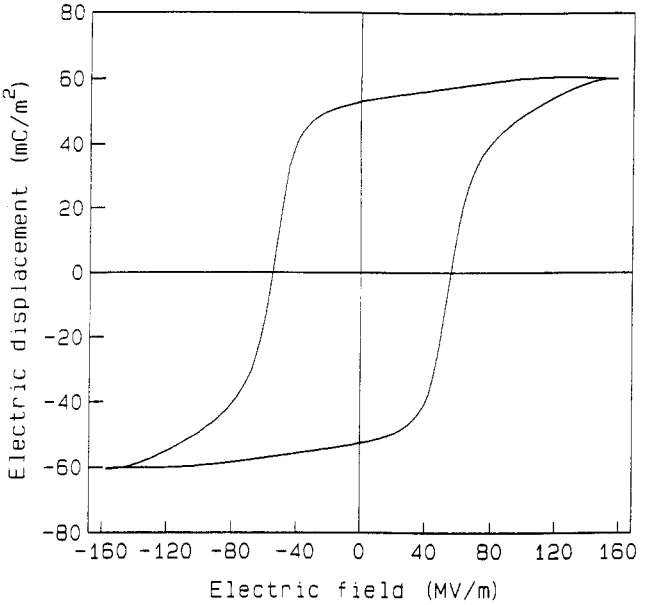

Figure 4. Electric displacement (D) versus electric field (E) for a drawn plus poled Nylon 11 film.

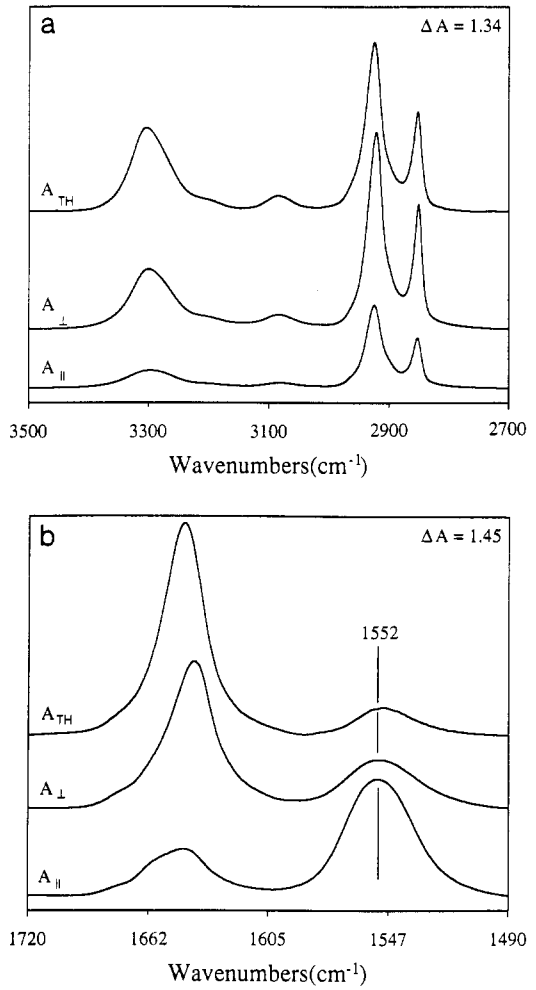

Figure 5. (a) Three-dimensional spectra of a drawn plus poled Nylon 11 film in the region 3500–2700 cm^{-1}. (b) Same as Figure 5a in the region 1720–1490 cm^{-1}.

The three-dimensional infrared spectra of a drawn, poled, and then annealed film are shown in Figure 6. A comparison with the poled sample in Figure 5 shows that the width of the amide A peak is narrowed and small intensity increases occur in both perpendicular and thickness directions. The amide I peak follows similar

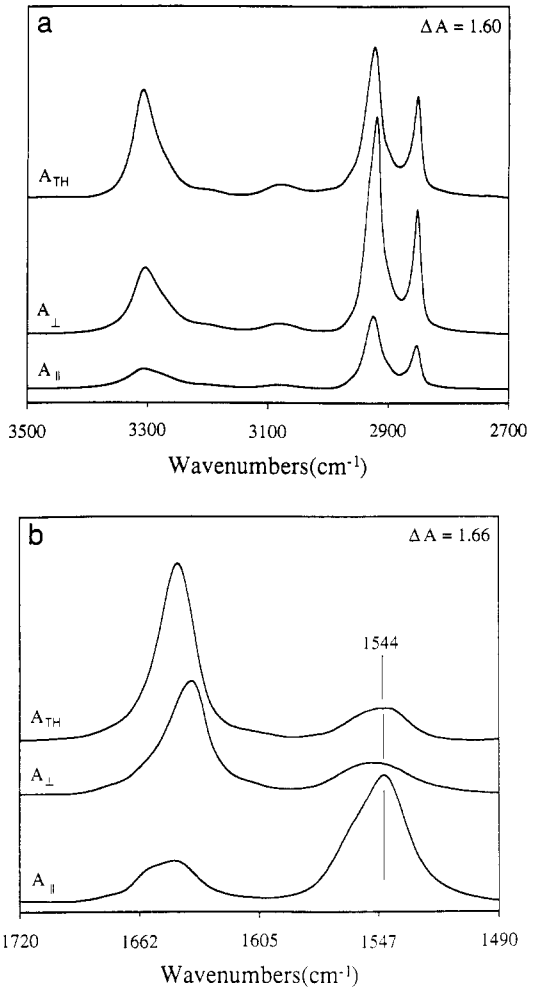

Figure 6. (a) Three-dimensional spectra of a drawn, poled, and then annealed Nylon 11 film in the region 3500–2700 cm^{-1}. (b) Same as Figure 6a in the region 1720–1490 cm^{-1}.

trends. The shift in the frequency of the amide II peak in the parallel direction from Figure 5b to 6b indicates that a phase transition from δ-like to α-like Nylon 11 crystals has occurred. A comparison of the amide A and I peaks of Figures 3 and 6 reveals that annealing after poling fixes the majority of the amide planes in the thickness direction, rather than in the perpendicular. The methylene stretching regions in Figures 3a and 6a show that the CH_2 units undergo changes in orientation between the annealed and the poled plus annealed films. In the poled plus annealed samples the intensity changes of the antisymmetric and symmetric peaks are consistent with a movement of the net CH_2 angle bisector toward the thickness direction in the drawn, poled, and then annealed film as compared with the drawn plus annealed film.

In general, polymer spectra consist of broad overlapping bands due to factors such as conformation, morphology, and intrachain phase relationships. Unless band profiles can be completely separated, the effect of the overlap by neighboring bands precludes the accurate determination of each absorbing species. This is certainly the case for those vibrational modes associated with the hydrogen-bonded functional groups of Nylon 11. We focus on two regions of the spectra of Nylon 11: the amide A region from 3500 to 3100 cm^{-1} and the amide I region from 1720 to 1600 cm^{-1}. According to Skrovanek et al.,[22] the N—H stretching mode is a composite band which does not contain separable features from ordered and disordered hydrogen-bonded conformations. In Figure 7 the absorption spectrum of an annealed film is shown on the bottom in the

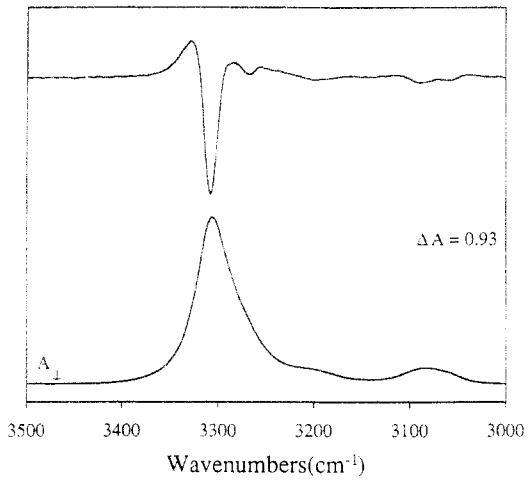

Figure 7. N—H stretching region of a drawn plus annealed film: (bottom) absorption spectrum in the perpendicular (X) direction; (top) unsmoothed second-derivative spectrum.

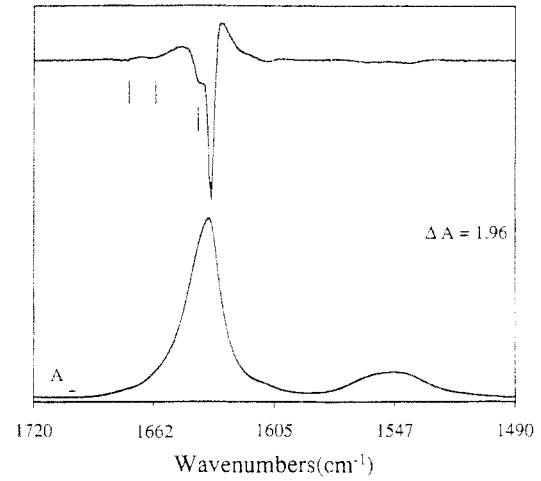

Figure 8. Bottom: perpendicular direction absorption spectrum for drawn plus annealed Nylon 11 film. Top: unsmoothed second-derivative spectrum.

perpendicular (X) direction. An obvious asymmetry occurs in the amide A peak ($\sim$3300 cm^{-1}) which shows up as a peak in the second-derivative spectrum above. The frequency of the (negative going) peak on the low-frequency side of the main peak in the second-derivative spectrum is around 3270 cm^{-1} and has been assigned as the amide I overtone.[18]

In contrast to the amide A peak, the amide I peak is a relatively complicated mode, separable into free (non-hydrogen-bonded) and disordered and ordered hydrogen-bonded structures. We initially attempted to curve-fit the amide I region with three bands, following the steps suggested by Coleman et al. for *in-situ* annealing of solvent cast Nylon 11 films.[19] However, the curve-fitting results were physically meaningless. After the issues involved were considered in some detail, the curve-fitting procedure delineated in Appendix A was adopted. Figure 9 shows an example of the result of the Gaussian curve-fitting procedure for an annealed film where the top spectrum in the bottom group is the sum of the Gaussian peaks. The top spectrum is the second derivative of the sum. The presence of four peaks in the amide I mode is clearly indicated in the second-derivative spectrum. An additional peak at $\sim$1610 cm^{-1} in both the experimental and synthesized data is currently unassigned. The existence of two disordered fractions or a total of four peaks in the second-derivative spectrum of the curve-fitting results is

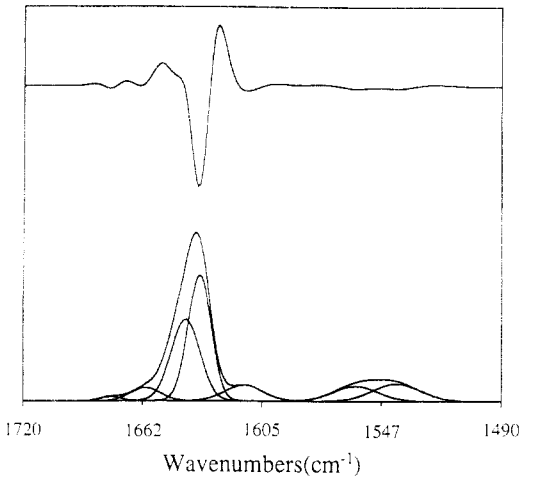

Figure 9. Bottom: least-squares Gaussian curve-fitting of the amide I–II region for a drawn plus annealed Nylon 11 film showing the sum of the Gaussian peaks. Top: second-derivative spectrum of the synthesized result.

Table 2. Relative Areas of the Curve-Fit Amide I Peak (%)

	sample treatment			
fraction	annealed ←	drawn →	poled →	poled + annealed
ordered	45.05 ± 2.07	32.15 ± 2.51	38.06 ± 1.89	45.15 ± 2.48
disordered (low $\bar{\nu}$)	42.82 ± 2.02	51.54 ± 2.90	43.72 ± 2.00	40.15 ± 2.10
disordered (high $\bar{\nu}$)	9.66 ± 0.48	12.42 ± 0.90	13.99 ± 1.07	11.83 ± 1.41
free	2.48 ± 0.22	4.17 ± 0.50	3.49 ± 0.24	3.06 ± 0.40

used in combination with the statistics of the curve-fitting process to choose fitting results which are physically meaningful and, at the same time, fix as few parameters as possible.

After collection of the polarized untilted and tilted film spectra, and the calculation of the A_z (thickness direction) spectrum, the amide I region of all spectra is curve-fitted. The spectra are processed to determine the relative amount of ordered, disordered, and free species independent of the orientation. The relative amount of ordered amide groups in Nylon 11 is found by summing the areas of the low-frequency ordered curve-fit peak in the three directions and dividing by the total amide I area in the three directions. The results are shown in Table 2, where all samples have been drawn and further treatments are as shown. The error on the given quantity is a result of at least two independently prepared samples and several curve-fitting trials which meet the criteria referred to earlier. This treatment yields $\sim$32% ordered material in the drawn Nylon 11. Annealing treatments increase the order to $\sim$45% as do poling plus annealing treatments. Poling of the drawn films increases the order by about 6%. These values are in the same range as that found with Nylon 11 solvent-cast from 1,1,1,3,3,3-hexafluoro-2-propanol, i.e., 34% at 30 °C.[19] The increase in the ordered fraction with the various treatments after drawing is mirrored by a decrease in the low-frequency disordered peak area, the free peak area, and to a less extent, the high-frequency disordered peak area. The implication of this result is that the ordered fraction increases at the expense of the free and both of the disordered fractions. The energetics of the low-frequency disordered hydrogen bonds are the most similar to that in the ordered phase, and it is, therefore, likely that ordered bonds are largely formed from this source, although we cannot prove this with the present results.

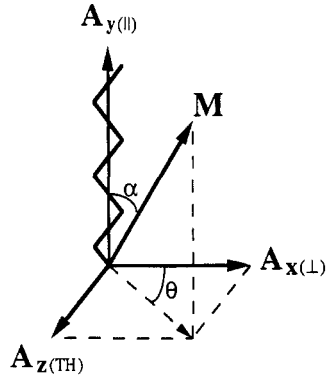

Figure 10. Transition dipole moment M in an axis system with orientation angles α and θ.

Once the curve-fitted intensities are determined for each direction, information about the orientation of the amide planes and the methylene spacers in the plane transverse to the draw direction can be obtained. A schematic of a representative transition dipole moment (M) is shown in Figure 10. The angle θ is defined as the orientation angle in the plane transverse to the draw direction (Y). Standard equations for the interaction of electromagnetic radiation with dipole moments can be applied. Starting with

$$A = C(\vec{\mathbf{E}}\cdot\vec{\mathbf{M}})^2 = (EM\cos\alpha)^2 \quad (2)$$

where A is the absorption intensity, C is a proportionality constant, and $\vec{\mathbf{E}}$ and $\vec{\mathbf{M}}$ are the electric and transition dipole moment vectors, respectively, anisotropy can be introduced as

$$A_{y(\|)} = (EM\cos\alpha)^2 \quad (3)$$

$$A_{x(\perp)} = (EM\sin\alpha\cos\theta)^2 \quad (4)$$

$$A_{z(\mathrm{TH})} = (EM\sin\alpha\sin\theta)^2 \quad (5)$$

Dividing eq 5 by eq 4 and rearranging yields

$$\theta = \tan^{-1}(A_z/A_x)^{1/2} \quad (6)$$

The use of eq 6 in conjunction with the curve-fitted intensities leads to information about the orientation of dipoles in the transverse plane. However, θ in eq 6 contains information about the orientation of the dipoles as well as the breadth of the orientation distribution. We will not attempt to make a separation at this point.

An orientation angle θ of 45° merits special consideration. 45° corresponds to either one of two indistinguishable conditions: (1) the dipoles projecting onto the plane transverse to the draw direction are randomly oriented or (2) the center of the orientation distribution is at 45° and the width of the distribution is of no consequence. Based on the sample treatments involved, driving forces exist which align the amide planes with the center of distribution of the transverse plane projections either in the perpendicular (X) direction (for simple one-way drawn or drawn plus annealed films) or in the thickness (Z) direction (for drawn plus poled or drawn, poled, and then annealed films). The potential for the formation of a bimodal distribution exists, particularly in the case of drawn plus poled films or drawn, poled, and annealed films. However, infrared spectroscopy cannot detect a bimodal distribution, but "sees" it as a unimodal distribution with its center between the bimodal maxima. In this case, the center of the distribution from infrared is along the X- or Z-axis, as in the case of a unimodal distribution. Returning to the significance of an orientation angle θ of 45° in the transverse plane, the occurrence of an orientation distribution of the amide planes with its center at 45° for drawn or drawn plus annealed films is highly unlikely since a driving force exists for amide plane alignment in the plane of the film. On the other hand, when the amide planes have a distribution centered in the plane of the film, the plane of the methylene spacers that bisects the CH_2 angle in the *all-trans* segment can have a bimodal distribution in the transverse plane. This is particularly true in Nylon 11 crystals where the plane of the amide group and the CH_2 bisector are not parallel.[2,5] Nonetheless, the angle between the planes would have to be close to 45° to be a problem in the present interpretations. This is not the case as reported in the literature. Again returning to a 45° orientation angle in the transverse plane, an ambiguity in the interpretation is introduced if 45° results for the amide planes after poling. In this case, a distinction between random orientation and a bimodal distribution with the modes centered at 45° cannot be made. With these caveats in mind we proceed to the analysis of θ.

Table 3. Orientation Angle θ (deg) of Amide Groups in the Transverse (X-Z) Plane

	sample treatment			
fraction	annealed ←	drawn →	poled →	poled + annealed
ordered	28.34 ± 1.46	35.92 ± 3.44	58.86 ± 2.20	49.63 ± 2.04
disordered (low $\bar{\nu}$)	48.10 ± 2.21	45.68 ± 1.49	47.34 ± 2.75	50.84 ± 2.05
disordered (high $\bar{\nu}$)	49.21 ± 2.88	49.31 ± 2.26	52.43 ± 3.17	47.41 ± 2.61
free	40.23 ± 3.74	51.37 ± 2.62	51.28 ± 3.73	52.94 ± 2.04

Table 4. Methylene Orientation Angle θ (deg) in the Transverse (X-Z) Plane

	sample treatment			
	annealed ←	drawn →	poled →	poled + annealed
$CH_2(\nu_a)_{obs}$	42.30 ± 1.27	45.07 ± 1.14	44.83 ± 1.48	40.47 ± 0.47
$CH_2(\nu_s)_{obs}$	38.83 ± 0.76	43.17 ± 1.17	43.80 ± 1.44	42.03 ± 0.78

Table 3 shows the values of θ derived from the curve-fitted amide I peak in the four sample treatments. In the drawn film, an angle of 35.9° for the ordered fraction establishes that the hydrogen-bonded sheets of the crystals of Nylon 11 in the transverse plane become aligned toward the plane of the film. This observation is in agreement with the work of Lee et al.,[7] Northolt,[8] and Chen et al.[14] The ordered fraction shows a substantial response to all postdrawing treatments, moving toward the plane of the film with annealing (θ = 28.3°) and toward the Z-axis (thickness direction) with poling (θ = 58.9°). Annealing treatments of the poled films show a tendency for the amide planes of the ordered fraction to move back to the plane of the film (θ = 58.9° → 49.6°). Other than the ordered fraction, all fractions show a small or negligible orientation response to the postdraw treatments (i.e., they remain random) or show a small tendency to orient toward the thickness direction.

In Table 4 the transverse plane orientation angle θ is shown for the methylene stretching peaks. The angles were found directly from the methylene stretching intensities, i.e., without curve-fitting. Since the ordered and disordered fractions cannot be separated in these peaks, the angles are a composite of all states of order. The table shows that the methylene units are random in the transverse plane as a result of drawing and drawing plus

poling treatments. A small amount of orientational order is introduced as a result of thermal treatments.

Discussion

The peak frequency of the N—H stretching peak around 3300 cm^{-1} is a sensitive indication of the average hydrogen bond strength in polyamides,[14,18,22] where high frequency corresponds to weaker bonds. Figure 11 shows the isotropic-equivalent spectra, $(A_x + A_y + A_z)/3$, for drawn (bottom) and drawn plus annealed (top) films. A comparison between the drawn and drawn plus annealed peak positions, 3300.0 and 3305.5 cm^{-1}, respectively, leads to the somewhat perplexing idea that the hydrogen bonding is weaker after annealing treatments. Table 1 also shows this for the three individual directions. We proceed with a discussion of this point.

Two prior works have shown that the amide A peak in Nylon 11[19] and a polyurethane[23] shifts up in frequency and reduces in intensity with *in-situ* heating, changes which correspond to the introduction of disorder in the hydrogen-bonded network. Similar changes in frequency were observed for the carbonyl stretching peak. Further, two other studies of *ex-situ* annealing of various types of polyurethanes[24,25] have shown that the N—H stretching peak width decreases and the frequency shifts downward after annealing. References 19 and 23–25 establish that during thermal treatments, the hydrogen bonds become weaker, corresponding to a large average distance associated with the bonds, wheres after annealing the average hydrogen-bond distance becomes smaller. The frequency changes observed in the present study are opposite to those previously published while the half-width changes follow similar trends. Two phenomena are discussed in order to shed light on the probable cause of frequency shifting of the N—H mode, Fermi resonance, and crystal phase changes.

Three low-intensity peaks occur in the N—H/CH_2 stretching region of the infrared spectrum shown in Figure 7, which are visible because of resonant interactions of amide I and II fundamentals with the N—H stretching fundamental. They are the amide I overtone at ~3270 cm^{-1}, the amide I + II combination mode at ~3200 cm^{-1}, and the amide II overtone at ~3080 cm^{-1}. In order to obtain information about Fermi resonant interactions independently of crystal phase changes, the two peaks which result from the phase-sensitive amide II mode are not considered. In order to address the initially stated problem of the increase in the N—H peak frequency with annealing treatments, we Gaussian curve-fit the 3400–3000 cm^{-1} region of the isotropic-equivalent spectra for three drawn and 3 drawn plus annealed films in order to determine the intensity of the amide I overtone. The peak positions were determined by the second or fourth derivatives and were fixed parameters in the fitting. Various features of the fitting and subsequent data treatment lead to the conclusion that the Fermi resonance in the drawn plus annealed films is weaker than in the drawn films. Those features are as follows. (1) The intensity of the (curve-fitted) amide I overtone peak is lower in the spectra of the annealed films. This change is coupled with an increase in the intensity of the amide I fundamental. (2) The equation[26]

$$\bar{\nu} = \frac{\bar{\nu}_1 + \bar{\nu}_2}{2} \pm \frac{\bar{\nu}_1 - \bar{\nu}_2}{2}\left(\frac{\rho - 1}{\rho + 1}\right) \qquad (7)$$

was used to predict the frequencies of the unperturbed ($\bar{\nu}$) amide I overtone and the N—H stretching fundamental

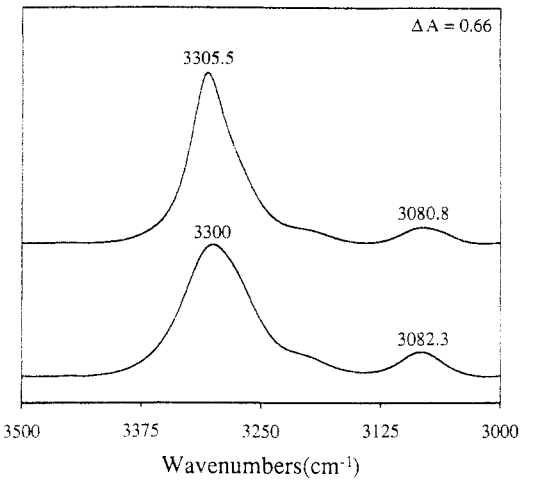

Figure 11. Amide A region of isotropic-equivalent spectra ($A_x + A_y + A_z$)/3: (bottom) drawn film; (top) drawn plus annealed film.

using the observed positions ($\bar{\nu}_i$) and the intensity ratio (ρ). This type of analysis is certainly limited by the fact that the N—H fundamental is also in resonance with the other two peaks in this region (mentioned just previously). Nonetheless, this treatment yields a smaller difference between the calculated unperturbed amide I overtone frequency and the observed frequency in the annealed films. (3) Again using eq 7, the difference between the calculated unperturbed amide I overtone frequency and the calculated unperturbed N—H fundamental frequency is larger in the drawn plus annealed films. Points 1–3 are consistent with stronger Fermi resonant interactions in the drawn films. However, the change in peak position and intensity of the observed N—H stretching peak in Figure 11 is inconsistent with a stronger resonance in the drawn film. It is concluded that resonance changes are not the cause of the higher frequency movement of the N—H fundamental in annealed film spectra.

Crystal phases in Nylon 11 can be categorized into triclinic (α, α') and pseudohexagonal (δ, δ', γ) structures. The latter has been described as possessing a shorter chain-axis repeat distance[5,27] which presumably contains more disorder in the methylene chain segments of the crystal phase. A distinction between triclinic and pseudohexagonal unit cells can easily be made with the 900–500 cm^{-1} region of the infrared spectra (amide V and VI region). Additionally, a variety of literature sources dealing with the infrared spectra of triclinic and pseudohexagonal crystal structures[3,4] as well as our own adjunct unpublished experimental work has established that the N—H stretching fundamental shifts about 5 cm^{-1} higher upon the γ- (or δ) to α-phase transition. Specifically, we have observed a 6 cm^{-1} increase, a 29% absorption intensity increase, and a decrease in the half-width as a result of annealing a trifluoroacetic acid-cast (γ-phase) film of Nylon 11. The same qualitative changes are observed in the isotropic-equivalent spectra between the drawn and drawn plus annealed films in this work (Figure 11). The conclusion that the increase in frequency of the N—H stretching peak upon annealing is due to a decrease in the hydrogen bond strength resulting from a crystal phase change is corroborated by the unit cell structures determined with X-ray diffraction (Table 2 of ref 28 and references therein). Whereas the δ and α transition produces a ~12% decrease in the inter-hydrogen bond sheet spacing (d_{010}), the interchain spacing within a sheet increases ~6% (d_{100}). The increase leads on the average to weaker hydrogen bonds after annealing treatments.

Table 5. Orientation Angle θ Calculated from Modeling Simulation

σ(HWHH) (deg)	height	$\theta_{\mu=0°}$ [a] (deg)	$\theta_{\mu=45°}$ (deg)	$\theta_{\mu=60°}$ (deg)	$\theta_{\mu=90°}$ (deg)
0	∞	0	45	60	90
11.46	1.9947	11.30	45.00	58.67	78.70
17.19	1.3298	16.68	45.00	56.65	73.32
22.92	0.9974	21.71	45.00	54.15	68.29
28.65	0.7992	26.23	45.00	51.98	63.77
34.38	0.6708	30.04	45.00	50.35	59.96
40.11	0.5844	33.04	45.00	49.16	56.96
45.84	0.5247	35.34	45.00	48.31	54.66
51.57	0.4823	37.10	45.00	47.69	52.90
57.30	0.4514	38.43	45.00	47.22	51.57
63.03	0.4283	39.49	45.00	46.86	50.51
∞	0.3183[b]	45	45	45	45

[a] μ = location of the center of the orientation distribution. [b] Height goes to a finite value due to integration limits.

As stated earlier in this work, two parameters affect the transverse plane orientation angle θ, i.e., the location of the center of the orientation distribution, and the breadth of the distribution. The parameters will be separated here in an attempt to learn more about the mechanism of polarization switching in Nylon 11. Using Figure 10 as a basis, the absorption intensity in any direction i can be written as

$$A_i = \int_{\theta=0}^{2\pi}\int_{\alpha=0}^{\pi/2}\mathbf{f}(\alpha,\theta)M_i^2\,d\alpha\,d\theta \tag{8}$$

where $\mathbf{f}(\alpha,\theta)$ is the three-dimensional distribution function of transition dipole moments. In this analysis we are concerned with the orientation in the transverse plane. The directional components of the dipole moment M can be written as

$$M_x = M\sin\alpha\cos\theta \tag{9}$$

$$M_z = M\sin\alpha\sin\theta \tag{10}$$

For the purpose of this analysis the angle α is set at $\pi/2$ and eq 8 in the transverse plane is

$$A_x = \int_0^{\pi/2}\mathbf{f}(\theta)M^2\cos^2\theta\,d\theta \tag{11}$$

$$A_z = \int_0^{\pi/2}\mathbf{f}(\theta)M^2\sin^2\theta\,d\theta \tag{12}$$

The upper limit on θ is taken as $\pi/2$ due to symmetry considerations. A Gaussian distribution function is assumed for $\mathbf{f}(\theta)$ where the center of the distribution (μ) can be adjusted as

$$\mathbf{f}(\theta) = \frac{a(\sigma)}{\sigma\sqrt{2\pi}}\exp\left(-\frac{1}{2}\left(\frac{\theta-\mu}{\sigma}\right)^2\right) \tag{13}$$

σ is the half-width at half-height and $a(\sigma)$ is related to the maximum intensity of $\mathbf{f}(\theta)$ as $a(\sigma) = \mathbf{f}(\theta)_{max}\sigma\sqrt{2\pi}$. Equations 11 and 12 can be used to find the absorption intensities along the principal symmetry axes and then eq 6 used to get θ. Using a normalized distribution function $\mathbf{f}(\theta)$, model calculations of θ are shown in Table 5 for a series of distribution half-widths and centers. As expected, when the center (μ) is at 45°, θ is independent of the half-width (σ), and when μ is not at 45°, θ depends on σ and μ.

At this point we proceed to an analysis of the polarization switching mechanism in Nylon 11. Of fundamental importance to the discussion is the observation that the amide planes of the ordered fraction tend to align in the plane of the film with one-way drawing, as evidenced by the value of θ in Table 3 (35.9°). It can be directly inferred, with reference to the transverse plane, that the axis along the center of the distribution of ordered amide planes lies in the plane of the film (on the X-axis). Therefore, μ = 0° in Table 5 and the width of the model Gaussian distribution for the ordered fraction of amide groups is ~46° (using θ = 35.9° from Table 3). Annealing of the ordered fraction decreases the value of θ to 28.3°, and using the same assumption that the center of distribution remains along the X-axis (μ = 0°), Table 5 indicates that the width of the distribution decreases to ~30°, as expected for an increase in ordering with annealing.

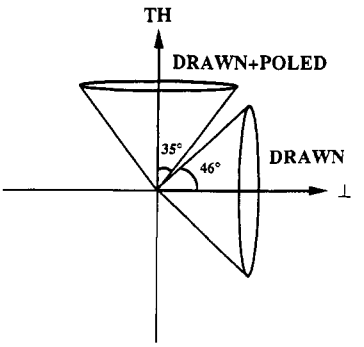

Figure 12. Schematic representation of the orientation distribution of ordered hydrogen-bonded amide planes before and after poling. The angle associated with each cone is the width of a model Gaussian orientation distribution function.

Two polarization switching mechanisms are considered for the ordered amide planes, 60 and 90° switching. These particular mechanisms are likely to be important in Nylon 11, the 60° switching due to the pseudohexagonal γ crystal phase which results upon drawing of melt-quenched Nylon 11 and the 90° due to the application of the electric field in a direction perpendicular to the center of distribution that results from drawing. For the purpose of argument, let us assume that the width of the distribution after drawing plus poling remains the same as after drawing only. According to Table 5, this condition leads to a θ value of ~48° for a 60° mechanism and ~54° for a 90° mechanism. The observed value of 58.9° (see Table 3 for the poled, ordered fraction) is considerably closer to the 90° switching. Further, in order for 60° switching to be operative, the width of the distribution would have to decrease to a value close to 0° in order to produce the experimentally observed orientation angle (θ) of 58.9°. The production of a narrow distribution of amide planes after electric field application is unlikely for two reasons: (1) a relatively broad distribution exists before field application (half-width = 46°) and (2) if a narrow distribution exists during the field application, the amide planes will relax after field removal in order to maximize hydrogen bond strength while minimizing conformational energetics. The 90° switching mechanism is suggested by this reasoning, given the liklihood of either 60 or 90° switching to be in operation. A schematic of the proposed switching is shown in Figure 12 where the cones represent the width of the model Gaussian orientation distribution for the ordered hydrogen-bonded amide planes. Further, according to Table 5, the width of the distribution decreases from 46 to 35° for the 90° mechanism, which is in accordance with the small increase in the ordered fraction upon poling shown in Table 2.

Conclusions

A trichroic FT-IR analysis of the amide groups in melt-quenched and cold-drawn Nylon 11 films has shown that

the amide groups tend to align in the plane of the film and that hydrogen bond strength is different along the three laboratory axes. The amide I band is resolved into four different species using derivative spectroscopy and Gaussian curve-fitting. Curve-fitting results of the amide I region show that the polarization switching behavior of Nylon 11 arises only from the ordered hydrogen-bonded domains. A Gaussian distribution model of infrared intensities is used to predict changes in the center and width of the transition dipole moment orientation distribution. The amide planes switch 90° from the original center of distribution in the drawn films in response to poling fields. Methylene units remain randomized with poling. The distribution of the amide group planes is narrowed with annealing treatments. The methylene segments and, specifically, the bisector of the CH_2 groups show a small rotation toward the plane of the film with annealing treatments and no movement with poling treatments.

Appendix A

1. Pseudobaseline Method. The choice of baseline is somewhat arbitrary. Nevertheless, when used in a systematic way it can sometimes give useful semiquantitative results. A linear baseline was included in the fitting procedure in the frequency range from 1720 to 1490 cm^{-1}, where no underlying absorbances are observed in this study.

2. Peak-Narrowing Method. The number of bands for curve-fitting in an experimental spectrum was determined by calculating the second, or fourth, derivative of the unresolved multiplet. An example is shown in Figure 8 for the perpendicular direction of a drawn plus annealed film. Minima in the second-derivative spectra indicate the presence of four peaks; the three higher frequency peaks are marked. We concluded that there are four different and resolvable states of hydrogen-bonded order contributing to amide I peak. The resolved peaks can be attributed to, from high wavenumbers to low, free carbonyl species (without hydrogen bonding), high- and low-wavenumber disordered hydrogen-bonded species, and ordered hydrogen-bonded domains.

3. Mathematical Equation Choice. The band shape in the infrared spectra of polymers can be characterized by Lorentzian or Gaussian functions, or a combination of both. In order to determine which mathematical function is suitable for this application, empirical tests were performed. Using the percentage of the Gaussian and Lorentzian bands as a variable in the initial testing, it was found that each resolved peak possessed at least 90% Gaussian character independent of the nature of the fit. Consequently, Gaussian bands shapes were used in all subsequent curve-fitting.

4. Least-Squares Gaussian Curve Fitting. Three parameters can be varied for each spectral feature: peak intensity, half-width at half-height, and peak position. In this application, the peak height and the half-width of the bands are varied, whereas peak positions are found from the second- or fourth-derivative spectra. Given the problems inherent in the curve-fitting process, a criterion beyond the use of fitting statistics was adopted. As noted above, four peaks exist in the second-derivative spectrum of the annealed film. In the second-derivative spectra of unannealed preparations, the shoulder is not as obvious, but its presence can be detected if its *a priori* existence is known. We use the presence of the shoulder as one of the criteria in the choice of acceptable fits. In other words, a visual comparison is made between the second-derivative spectrum of the synthesized result and the second-derivative spectrum of the experimental spectrum. A good match between the two was found by controlling the extent of the minimization process.

References and Notes

(1) Schmidt, G. F.; Stuart, H. A. *Z. Naturforsch.* **1958**, *13A*, 222.
(2) Slichter, W. P. *J. Polym. Sci.* **1959**, *35*, 77.
(3) Saski, T. *J. Polym. Sci., Part B: Polym. Lett.* **1965**, *3*, 557.
(4) Kinoshita, Y. *Makromol. Chem.* **1959**, *33*, 1.
(5) Newman, B. A.; Sham, T. P.; Pae, K. D. *J. Appl. Phys.* **1977**, *48*, 4092.
(6) Lee, J. W.; Takase, Y.; Newman, B. A.; Scheinbeim, J. I. *J. Polym. Sci., Part B: Polym. Phys.* **1991**, *29*, 273.
(7) Lee, J. W.; Takase, Y.; Newman, B. A.; Scheinbeim, J. I. *J. Polym. Sci., Part B: Polym. Phys.* **1991**, *29*, 279.
(8) Northolt, M. G. *J. Polym. Sci., Part C: Polym. Symp.* **1972**, *38*, 205.
(9) Scheinbeim, J. I.; Lee, J. W.; Newman, B. A. *Macromolecules* **1992**, *25*, 3729.
(10) Schmidt, P. G. *J. Polym. Sci., Part A: Gen. Pap.* **1963**, *1*, 1271.
(11) Fina, L. J.; Koenig, J. L. *J. Polym. Sci., Part B: Polym. Phys.* **1986**, *24*, 2509.
(12) Fina, L. J.; Koenig, J. L. *J. Polym. Sci., Part B: Polym. Phys.* **1986**, *24*, 2525.
(13) Fina, L. J.; Koenig, J. L.; Gordon, W. L. *J. Polym. Sci., Part B: Polym. Phys.* **1986**, *24*, 2541.
(14) Chen, G. C.; Su, J.; Fina, L. J. *J. Polym. Sci., Part B: Polym. Phys.*, submitted for publication.
(15) Kohan, M. I., ed. *Nylon plastics*; John Wiley & Sons: New York, 1973; p 396.
(16) Moore, W. H.; Krimm, S. *Biopolymers* **1976**, *15*, 2439.
(17) Miyazawa, T. *J. Chem. Phys.* **1960**, *32* (6), 1647.
(18) Fina, L. J.; Yu, H. H. *J. Polym. Sci., Part B: Polym. Phys.* **1992**, *30*, 1073.
(19) Skrovanek, D. J.; Painter, P. C.; Coleman, M. M. *Macromolecules* **1986**, *19*, 699.
(20) Arimoto, H. *J. Polym. Sci., Part A: Gen. Pap.* **1964**, *2*, 2283.
(21) Bradbury, E. M.; Elliot, A. *Polymer* **1963**, *4*, 47.
(22) Skrovanek, D. J.; Howe, S. E.; Painter, P. C.; Coleman, M. M. *Macromolecules* **1985**, *18*, 1676.
(23) Coleman, M. M.; Lee, K. H.; Skrovanek, D. J.; Painter, P. C. *Macromolecules* **1986**, *19*, 2149.
(24) Brunette, C. M.; Hsu, S. L.; MacKnight, W. J. *Macromolecules* **1982**, *15*, 71.
(25) Pollack, S. K.; Shen, D. Y.; Hsu, S. L.; Wang, Q.; Stidham, H. D. *Macromolecules* **1989**, *22*, 551.
(26) Colthup, N. B.; Daly, L. H.; Wiberley, S. E. *Introduction to Infrared and Raman Spectroscopy*, 2nd ed.; Academic Press: New York, 1975; p 29.
(27) Chen, P. K.; Newman, B. A.; Scheinbeim, J. I. *J. Mater. Sci.* **1985**, *20*, 1753.
(28) Mathias, L. J.; Powell, D. G.; Autran, J. P.; Porter, R. S. *Macromolecules* **1990**, *23*, 963.